Available online at www.sciencedirect.com

ScienceDirect

IFAC Papers Online CONFERENCE PAPER ARCHIVE

IFAC PapersOnLine 55-37 (2022) 56–61

Extremum-Seeking-Based Ultra-local Model Predictive Control and Its Application to Electric Motor Speed Regulation

Yujing Zhou * **Zejiang Wang** ** **Xingyu Zhou** ***
Heran Shen *** **Jin Ahn** *** **Junmin Wang** ***

* *Department of Mechanical and Aerospace Engineering, Princeton University, Princeton, NJ 08544, USA (e-mail: yz1324@princeton.edu).*
** *Oak Ridge National Laboratory, Oak Ridge, TN 37830, USA (e-mail: wangzejiang@utexas.edu)(corresponding author)*
*** *Walker Department of Mechanical Engineering, The University of Texas at Austin, Austin, TX 78758 USA , (e-mail: xingyu.zhou@utexas.edu, hs29354@utexas.edu, hjahn@utexas.edu, jwang@austin.utexas.edu)*

Abstract: Electric vehicle (EV) market is rapidly expanding. As a critical component of EV, an electric motor needs to accurately follow a reference speed signal while respecting the electrical current constraint for safety. Those requirements are usually formulated as a model predictive control (MPC) problem. However, the performance of traditional model-based MPC depends on the accuracy of the system model, which may not always be guaranteed in reality. Therefore, we utilize a data-driven, model-free predictive control strategy, called ultra-local MPC (ULMPC), to control the speed of an electric motor. To further enhance the control performance of ULMPC, we employ the extremum-seeking control (ESC) to tune the control gain of the ULMPC online. Simulation and hardware experiments demonstrate the enhancement of the extremum-seeking-based ULMPC over a constant-gain ULMPC.

Keywords: Electric motor, electric vehicle, extremum-seeking control, model-free control.

1. INTRODUCTION

Thanks to the higher efficiency, lower emission, and quieter operation, electric vehicles (EV) have witnessed explosive popularity in the last decade (Crolla and Cao (2012)). As a critical component of EV, electric motors need to accurately follow the reference speed while respecting the motor electrical current constraint for safety. Model-predictive control (MPC) is frequently employed to deal with such a constrained optimal control problem (Vafamand et al. (2018)). However, the control performance of MPC heavily depends on the accuracy of the system model. Unfortunately, accurate electric motor models are hard to obtain because they rely on several time-varying and hard-to-measure parameters, such as temperature and demagnetization (Ruoho et al. (2009)). To bypass the requirement of an accurate model, we employ the newly developed ultra-local model predictive control (ULMPC) (Wang and Wang (2020)), which is a data-driven, model-free predictive control strategy, to control the electric motor speed following a varying reference signal under its current magnitude constraint.

Even though the effectiveness and ease of implementation of ULMPC have already been experimentally demonstrated (Wang and Wang (2020)), tuning the critical control gain of ULMPC remains largely a trial-and-error process and can be both time-consuming and poorly performing. Indeed, finding a systematic method for tuning this hyperparameter is actively under investigation (Fliess and Join (2021)). Recently, some researchers proposed to online adjust the control gain based on the last-step control command, but the tuned control gain can suffer from drastic oscillation (Doublet et al. (2016), Polack et al. (2017)).

Inspired by our recent work (Wang et al. (2022b)), we introduce the extremum-seeking control (ESC) into the ULMPC framework. ESC employs the averaging theory to estimate the local gradient of a predefined cost function w.r.t. the control gain of the ULMPC, without knowing the explicit mathematical relationship between the two variables. Based on the estimated gradient information, we then use gradient descent to continuously update the control gain online, with the purpose of progressively improving the control performance of an ULMPC.

The rest of this paper is organized as follows. In Section 2, we briefly review ULMPC and then illustrate how to apply ULMPC for electric motor speed control. Afterward, we illustrate in Section 3 how to integrate ESC with the ULMPC to tune the control gain of the latter online, which yields the extremum-seeking based ultra-local model predictive control (ES-ULMPC). In Section 4 and Sec-

10.1016/j.ifacol.2022.11.161

tion 5, simulation and hardware experiments respectively demonstrate the performance enhancement of the ES-ULMPC over a constant-gain ULMPC in electric motor speed control. Finally, Section 6 concludes this paper.

2. ULTRA-LOCAL MODEL PREDICTIVE CONTROL

This section briefly reviews the ULMPC, which was first proposed in our work (Wang and Wang (2020)).

2.1 Ultra-local Model

In contrast to traditional model-based predictive controllers (Wang et al. (2019), Quirynen and Di Cairano (2020), Chen and Wang (2015), Zhao and Wang (2016)), which rely on a physical model to predict the states of the controlled plant within the prediction horizon, ULMPC represents the controlled plant as its ultra-local model. The ultra-local model expresses the derivative of the system output as the sum of the amplified system input and an offset term. Mathematically speaking, we have (Fliess and Join (2013)):

$$y^{(\nu)}(\tau) = F(\tau) + \alpha u(\tau), \tag{1}$$

where $y^{(\nu)}(\tau)$ is the $\nu-th$ order derivative of the measured system output $y(\tau)$, $\alpha u(\tau)$ represents the amplified system input $u(\tau)$, α is a constant control gain, and $F(\tau)$ is the offset term, which groups both the unmodeled system dynamics and the external disturbances. $F(\tau)$ is regarded as a piecewise constant.

To ensure that the ultra-local model can represent the dynamics of the controlled plant within a short period, we continuously update $F(\tau)$ at each sampling step, as:

$$F(\tau) \approx \hat{F}(\tau) = \hat{y}^{(\nu)}(\tau) - \alpha u(\tau - T_s), \tag{2}$$

where $u(\tau - T_s)$ is the command at the last step, with T_s as the sampling period. $\hat{y}^{(\nu)}(\tau)$ is the estimated $\nu - th$ order derivative of the measured system output $y(\tau)$. In practice, we employ the algebraic derivative estimation (ADE) (Mboup et al. (2009)) to formulate the derivative of $y(\tau)$ via its time-weighted integral. For instance, we can express $\hat{\dot{y}}(\tau)$ as:

$$\hat{\dot{y}}(\tau) = \frac{6}{T_{ADE}^3} \int_0^{T_{ADE}} (T_{ADE} - 2t) y(\tau - t) dt, \tag{3}$$

where T_{ADE} is typically set as an integer multiple of T_s for digital implementation. Note that instead of amplifying the measurement noises from direct differentiation, the integral serves as a low-pass filter to mitigate the measurement noises. Substituting (2) into (1) yields:

$$\begin{aligned} y^{(\nu)}(\tau) &\approx \hat{y}^{(\nu)}(\tau) - \alpha u(\tau - T_s) + \alpha u(\tau) \\ &= \hat{y}^{(\nu)}(\tau) + \alpha \Delta u(\tau), \end{aligned} \tag{4}$$

where $\Delta u(\tau)$ is the control increment at the current step. In (4), we have $\nu = 1$ in general (Fliess and Join (2013)). However, the tuning of the control gain α remains an open problem (Fliess and Join (2021)).

2.2 Predictive Control Based on the Ultra-local Model

Assuming $\nu = 1$ in (4), we can discretize (4) as:

$$y_{k+1|k} = y_{k|k} + T_s \hat{\dot{y}}(k) + \alpha T_s \Delta u_{k|k}, \tag{5}$$

where $y_{k|k}$ represents the measured system output at the current step. $y_{k+1|k}$ indicates the predicted system output at the next step. $\Delta u_{k|k}$ is the control increment at the current step. The cost function to minimize can be expressed as:

$$J = \sum_{i=1}^{H_p} \|y_{k+i|k} - y_{k+i|k}^r\|_Q^2 + \sum_{i=0}^{H_c-1} \|\Delta u_{k+i|k}\|_R^2, \tag{6}$$

where $y_{k+i|k}$ and $y_{k+i|k}^r$ represent respectively the predicted system output and its reference within the prediction horizon H_p, $\Delta u_{k+i|k}$ indicate the successive control increments within the control horizon H_c, and Q and R are weighting factors. The first term penalizes the tracking error, while the second term punishes drastic control variations.

Meanwhile, the system constraints include:

(a) The restraints on the control increments:

$$\begin{cases} -\Delta U_{max} \le \Delta u_{k+i|k} \le \Delta U_{max} & i = 0, ..., H_c - 1, \\ \Delta u_{k+i|k} = 0 & i = H_c, ..., H_p, \end{cases} \tag{7}$$

where ΔU_{max} corresponds to the maximum control increment.

(b) The limits on the control magnitude:

$$\begin{cases} U_{min} \le U(k-1) + \sum_{i=0}^{n} \Delta u_{_{k+i|k}} \le U_{max}, & n = 0, \\ \quad \vdots \\ U_{min} \le U(k-1) + \sum_{i=0}^{n} \Delta u_{_{k+i|k}} \le U_{max}, & n = H_c - 1, \end{cases} \tag{8}$$

with U_{max} and U_{min} as the upper and lower bounds on the actuator output and $U(k-1)$ as the control at the last step.

(c) The constraints on the predicted system output:

$$y_{min} \le y_{k+i|k} \le y_{max}, \quad i = 1, ..., H_p. \tag{9}$$

Minimizing (6) under (7)-(9) yields the optimal control increment series at step k. Denoting the first element of the optimized increment series as $\Delta u_{k|k}^*$, the optimal control at the current step k reads:

$$U^*(k) = U(k-1) + \Delta u_{k|k}^*. \tag{10}$$

2.3 Electric Motor Speed Control via ULMPC

We apply the ULMPC for electric motor speed regulation. We first formulate the ultra-local model of an electric motor as:

$$\begin{cases} \dot{w}(t) = F_w(t) + \alpha_w I(t), \\ \dot{I}(t) = F_I(t) + \alpha_I u(t), \end{cases} \tag{11}$$

where $w(t)$ is the motor angular velocity, $I(t)$ is the motor current, and $u(t)$ represents the system input, which can be voltage or normalized throttle input from a driver. $F_w(t)$ and $F_I(t)$ are the offset terms. α_w and α_I are control gains.

From (4), the corresponding incremental ultra-local model with respect to (11) is:

$$\begin{cases} \dot{w}(t) = \hat{\dot{w}}(t) + \alpha_w \Delta I(t), \\ \dot{I}(t) = \hat{\dot{I}}(t) + \alpha_I \Delta u(t). \end{cases} \tag{12}$$

In (12), $\hat{\dot{w}}(t)$ and $\hat{\dot{I}}(t)$ are the algebraically estimated derivatives from (3). $\Delta I(t)$ and $\Delta u(t)$ are the current increment and control increment, respectively. Since $\Delta I(t) \approx \dot{I}(t)T_s$, we can express the first equation in (12) as:

$$\dot{w}(t) = \hat{\dot{w}}(t) + \alpha_w \hat{\dot{I}}(t) T_s + \alpha_I \alpha_w T_s \Delta u(t). \tag{13}$$

Replacing the first equation in (12) by (13), we obtain:

$$\begin{bmatrix} \dot{I}(t) \\ \dot{w}(t) \end{bmatrix} = \begin{bmatrix} \hat{\dot{I}}(t) \\ \hat{\dot{w}}(t) + \alpha_w T_s \hat{\dot{I}}(t) \end{bmatrix} + \begin{bmatrix} \alpha_I \\ \alpha_I \alpha_w T_s \end{bmatrix} \Delta u(t). \tag{14}$$

We discretize (14) with the sampling period T_s, and obtain:

$$\begin{bmatrix} I_{k+1|k} \\ w_{k+1|k} \end{bmatrix} = \begin{bmatrix} I_{k|k} \\ w_{k|k} \end{bmatrix} + \begin{bmatrix} \hat{\dot{I}}(k) T_s \\ \hat{\dot{w}}(k) T_s + \alpha_w \hat{\dot{I}}(k) T_s^2 \end{bmatrix} + \begin{bmatrix} \alpha_I T_s \\ \alpha_I \alpha_w T_s^2 \end{bmatrix} \Delta u_{k|k}, \tag{15}$$

where $I_{k|k}$ and $w_{k|k}$ are the measured current and motor angular velocity at the current step, $I_{k+1|k}$ and $w_{k+1|k}$ represent the one-step-predicted current and motor angular velocity, and $\Delta u_{k|k}$ is the control increment at the current step.

With (15), the motor speed control problem under the constraint of the maximal current can be formulated in (16). The first term in the cost function aims to minimize the angular velocity tracking error within the prediction horizon. The second term penalizes drastic control fluctuation within the control horizon. The third term, which is optional only, tries to match the current step command with a feedforward command $U^r(k)$. $U^r(k)$ can be derived from system inversion (Wang et al. (2020)).

Then, the first constraint corresponds to the system dynamics. The second and third constraints limit the control increments. The fourth constraint restrains the predicted motor current within the prediction horizon. The rest of the constraints limit the control magnitude, with U_{max} being the maximum actuator output.

This quadratic programming problem can be efficiently solved, which yields the optimal control increment series $\Delta u^*_{k+i|k}$. Finally, the optimal command at the current step is expressed in (10).

$$\arg \min_{\Delta u_{k+i|k}} J_{MPC} = \sum_{i=1}^{H_p} \|w_{k+i|k} - w^r_{k+i|k}\|^2_Q + \sum_{i=0}^{H_c-1} \|\Delta u_{k+i|k}\|^2_{R_1} + \|U^*(k) - U^r(k)\|^2_{R_2}$$

s.t.

$$\begin{cases} \begin{bmatrix} \dot{I}_{k+1|k} \\ \dot{w}_{k+1|k} \end{bmatrix} = \begin{bmatrix} \hat{\dot{I}}_{k|k} \\ \hat{\dot{w}}_{k|k} \end{bmatrix} + \begin{bmatrix} \hat{\dot{I}} T_s \\ \hat{\dot{w}} T_s + \alpha_w \hat{\dot{I}} T_s^2 \end{bmatrix} + \begin{bmatrix} \alpha_I T_s \\ \alpha_I \alpha_w T_s^2 \end{bmatrix} \Delta u_{k|k}, & i = 0, ..., H_p, \\ -\Delta U_{max} \le \Delta u_{k+i|k} \le \Delta U_{max}, & i = 0, ..., H_c - 1, \\ \Delta u_{k+i|k} = 0, & i = H_c, ..., H_p, \\ 0 \le I_{k+i|k} \le I_{max}, & i = 1, ..., H_p + 1, \\ U_{min} \le U(k-1) + \sum_{i=0}^{n} \Delta u_{k+i|k} \le U_{max}, & n = 0, \\ \vdots & \vdots \\ U_{min} \le U(k-1) + \sum_{i=0}^{n} \Delta u_{k+i|k} \le U_{max}, & n = H_c - 1. \end{cases} \tag{16}$$

Remark: Algebraically estimating the derivative of system output introduces estimation error (Wang et al. (2022a)). As a consequence, ULMPC can merely guarantee practical stability instead of asymptotic stability.

3. EXTREMUM-SEEKING-BASED ULTRA-LOCAL MODEL PREDICTIVE CONTROL

Manually tuning the control gains α_w and α_I in (11)-(15) could be painstaking and poorly performing. Therefore, we propose to employ the extremum-seeking control (ESC) (Krstic and Wang (1998)) to continuously tune α_w and α_I online. Note that ESC has been applied for tuning PID controller (Killingsworth and Krstic (2006)), model-based predictive controller (Tran et al. (2014)), and Model-Free Controller (Wang et al. (2022b)). However, to the best of our knowledge, this work pioneers applying ESC to tune the control gain of ULMPC.

3.1 Gain Tuning via Extremum-Seeking Control

ESC tries to minimize a cost function $J_{ESC}(\alpha)$, without knowing the explicit relationship between the cost function J_{ESC} and the optimized variable α. To this end, ESC first estimates the gradient $\partial J_{ESC}/\partial \alpha$ and then updates α such that $J_{ESC}(\alpha)$ converges towards a local minimum.

To estimate $\partial J_{ESC}/\partial \alpha$, ESC perturbs α with a sinusoidal signal $\Delta\alpha \sin(w_{ESC}t)$, termed as dither, and observes the variation of the cost function under the influence of the dither. By use of the first-order Taylor expansion, we have:

$$\begin{aligned} &J_{ESC}(\alpha + \Delta\alpha \sin(w_{ESC}t)) \\ &= J_{ESC}(\alpha) + \Delta\alpha \frac{\partial J_{ESC}}{\partial \alpha} \sin(w_{ESC}t) + O(\Delta^2 \alpha^2 \sin^2(w_{ESC}t)), \end{aligned} \tag{17}$$

where $O(\cdot)$ condenses the higher-order terms, and it is omitted in the sequel for simplicity. Multiplying (17) with a unit dither $\sin(w_{ESC}t)$ yields:

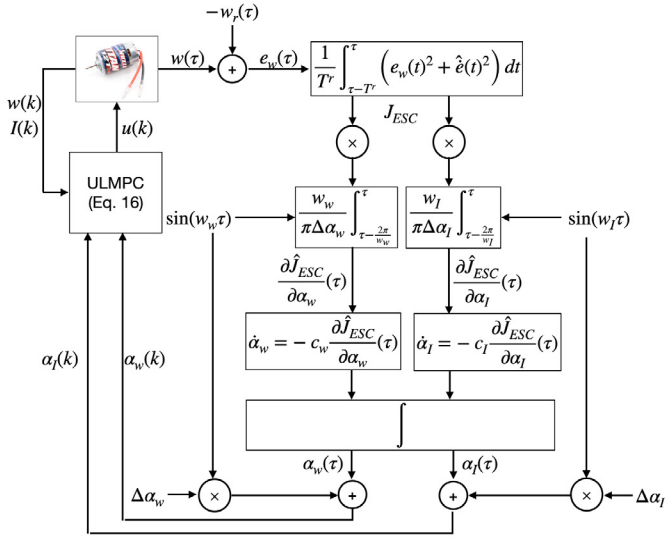

Fig. 1. Extremum-seeking-based ULMPC.

$$\begin{aligned}\mu(t) &= J_{ESC}(\alpha)\sin(w_{ESC}t) + \Delta\alpha\frac{\partial J_{ESC}}{\partial\alpha}\sin^2(w_{ESC}t)\\ &= J_{ESC}(\alpha)\sin(w_{ESC}t) + \frac{\Delta\alpha}{2}\frac{\partial J_{ESC}}{\partial\alpha}(1-\cos(2w_{ESC}t)).\end{aligned} \tag{18}$$

To remove the harmonic components in (18), we average $\mu(t)$ over a period of the dither, as:

$$\mu_{avg}(t) = \frac{w_{ESC}}{2\pi}\int_{t-\frac{2\pi}{w_{ESC}}}^{t}\mu(\tau)d\tau = \frac{\Delta\alpha}{2}\frac{\partial J_{ESC}}{\partial\alpha}. \tag{19}$$

Therefore, the approximated gradient becomes:

$$\frac{\partial J_{ESC}}{\partial\alpha}(t) = \frac{2}{\Delta\alpha}\mu_{avg}(t). \tag{20}$$

Finally, the optimized variable α can be updated as:

$$\dot{\alpha}(t) = -c\frac{\partial J_{ESC}}{\partial\alpha}(t), \tag{21}$$

with $c > 0$ to drive J_{ESC} to a local minimum.

3.2 ES-ULMPC for Electrical Motor Speed Control

Employing (17)-(21) to update the control gains α_w and α_I in (16) yields the extremum-seeking-based ultra-local model predictive control (ES-ULMPC). The framework of ES-ULMPC is illustrated in Fig. 1.

In Fig. 1, the cost function for ESC to minimize is:

$$J_{ESC} = \frac{1}{T^r}\int_{\tau-T^r}^{\tau}\left(e_w(t)^2 + \hat{e}_w(t)^2\right)dt, \tag{22}$$

which includes the motor speed tracking error $e_w(t) = w(t) - w^r(t)$ and its derivative within the past T^r seconds. If the reference speed $w^r(t)$ maintains periodicity, T^r can be set as its period (Hunnekens et al. (2014)). In (16), there exist two control gains α_w and α_I to tune. Therefore, J_{ESC} passes through two channels in parallel to update $\alpha_w(\tau)$ and $\alpha_I(\tau)$ simultaneously. Parameters tuning of the multi-variable ESC, including the dither amplitudes $\Delta\alpha_w$, $\Delta\alpha_I$, dither frequencies w_w, w_I, and update gains c_w, c_I follows the guidelines in (Hunnekens et al. (2014)) and (Ghaffari et al. (2012)). In particular, we set the sampling periods of both the MPC and the ESC equally to $0.01s$. As a consequence, we assume that the control gains $\alpha_w(k)$ and $\alpha_I(k)$ remain unchanged within the prediction horizon at each MPC sampling step.

Remark: J_{ESC} in (22) is built upon the recorded tracking errors in the *past*, while J_{MPC} in (16) is constructed with the predicted tracking errors in the *future*.

4. SIMULATION RESULTS

We first demonstrate the control performance enhancement of the ES-ULMPC over an ULMPC with constant control gains.

4.1 Model of the Simulated Electrical Motor

The electric motor model from the hardware vendor reads:

$$\begin{cases} U = R_{elec}I + K_{elec}w, \\ K_{elec}I = J_{elec}\dot{w} + B_{elec}w + C_{elec}|\dot{w}|, \end{cases} \tag{23}$$

where U is the voltage applied to the electric motor, I and w, identical to (11), correspond to the motor current and the motor angular velocity, and R_{elec}, K_{elec}, J_{elec}, B_{elec}, C_{elec} are motor parameters. Based on (23), we can express the relationship between the command U and the angular velocity w as:

$$U = R_{elec}(J_{elec}\dot{w} + B_{elec}w + C_{elec}|\dot{w}|)/K_{elec} + K_{elec}w. \tag{24}$$

With the reference speed w^r and the nominal motor parameters: R^0_{elec}, K^0_{elec}, J^0_{elec}, B^0_{elec}, C^0_{elec}, the feedforward command U^r in (16) can be expressed as:

$$U^r = R^0_{elec}(J^0_{elec}\dot{w}_r + B^0_{elec}w_r + C^0_{elec}|\dot{w}_r|)/K^0_{elec} + K^0_{elec}w_r. \tag{25}$$

Remark: Like other model-free algorithms, knowing some system dynamics, even though not required, can benefit the ES-ULMPC.

4.2 Simulation Results

The reference speed w_r is a sinusoidal signal with varying frequencies and magnitudes, as:

$$\begin{cases} w_r(t) = 413 + 113.35\sin(t), & t \le 1000, \\ w_r(t) = 413 + 135.75\sin(t), & t > 1000. \end{cases} \tag{26}$$

Per (Hunnekens et al. (2014), Ghaffari et al. (2012)), T^r in (22) is fixed as 2π, the nominal control gains are set as $\alpha_I(0) = 60000$ and $\alpha_w(0) = 10000$, and the dither amplitudes $\Delta\alpha_w$ and $\Delta\alpha_I$ are 3% of their nominal values. The dither frequencies are $w_I = 0.2rad/s$ and $w_w = 0.25rad/s$. Then, in (16), the prediction horizon is $H_p = 20$ and the control horizon is $H_c = 1$. The maximum current is $I_{max} = 0.85A$. The maximum input and input increment

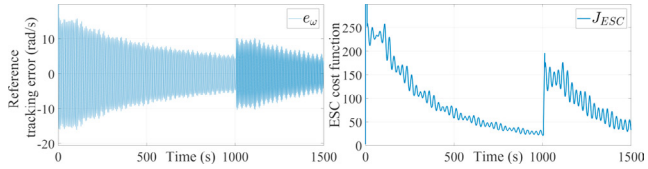

Fig. 2. Reference tracking error and ESC cost function.

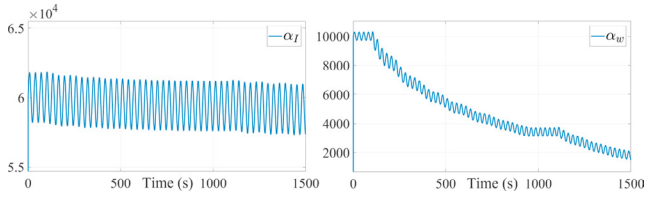

Fig. 3. Control gains profile from simulation.

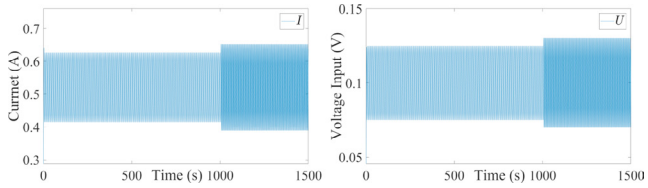

Fig. 4. Motor current and voltage.

are $U_{max} = 0.15$ and $\Delta U_{max} = 0.01$, respectively. Finally, the weighting factors are $Q = 16$, $R_1 = 10$, and $R_2 = 1$. Note that R_2 is set relatively small because the accuracy of the inversed model (25) is not guaranteed.

We first show that with the control gains α_I and α_w being continuously updated by ESC, the ES-ULMPC can demonstrate a progressively improved tracking performance. Based on (26), the ESC is enabled at $100s$ after the motor has entered its steady state. Moreover, we disable the ESC at $1000s$ and re-activate it at $1100s$ to handle the reference variation. The reference speed tracking error and J_{ESC} are demonstrated in Fig. 2.

Before ESC is enabled, the ULMPC with constant control gains yields a tracking error $e_w(t)$ above $13rad/s$, which induces a large J_{ESC}. After ESC is activated at $100s$, $e_w(t)$ gradually reduces to less than $5rad/s$. However, facing the sudden change of the reference speed $w_r(t)$ at 1000s, $e_w(t)$ rebounds to $10rad/s$. With ESC being enabled again at 1100s, $e_w(t)$ gradually reduces to $6rad/s$, along with a reduced J_{ESC}.

The control gains are demonstrated in Fig. 3. α_I remains close to its initial value, probably because the gradient $\partial J_{ESC}(\alpha_I, \alpha_w)/\partial \alpha_I|_{\alpha_I=60000} \approx 0$. Instead, α_w reduces from 10000 to 3500 before $1000s$, and further decreases from 3500 to 2000 after $1100s$, which yields a reduced $e_w(t)$ and J_{ESC} in Fig. 2.

The motor current I and voltage U are shown in Fig. 4, with the constraints: $I < I_{max} = 0.85$ and $U < U_{max} = 0.15$ being always satisfied.

5. EXPERIMENTAL RESULTS

We further implement the ES-ULMPC on a brushed DC motor. We first describe the experimental setup and then demonstrate the experimental results.

Fig. 5. Brushed DC motor used in the experimentation.

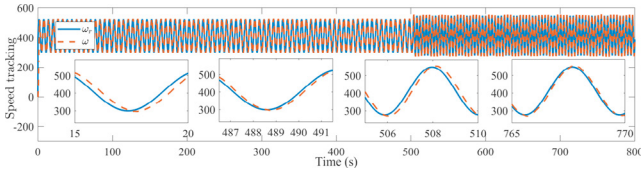

Fig. 6. Motor speed tracking result.

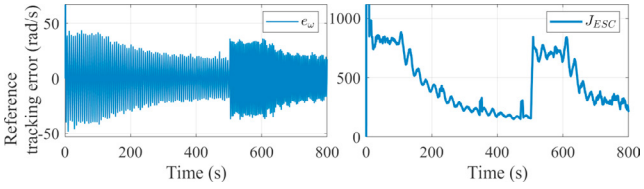

Fig. 7. Motor speed tracking error and ESC cost function.

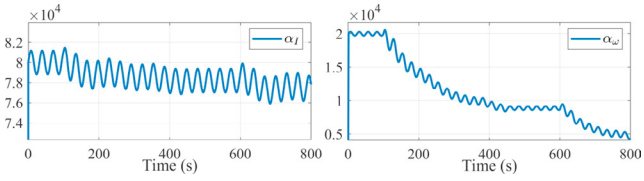

Fig. 8. Control gains profile from experiments.

5.1 Experimental Setup

As shown in Fig. 5, the controlled plant is a Traxxas brushed DC motor embedded in a Quanser QCar. An encoder measures the motor angular velocity w. QUARC firmware measures the motor current I and inputs a normalized throttle command U to the motor.

Similar to (26), the reference speed is a sinusoidal signal with piecewise constant frequencies and magnitudes.

5.2 Experimentation Results

The reference tracking result is exhibited in Fig. 6. As shown in the enlarged insets, the ES-ULMPC progressively improves the tracking performance. This fact is validated again in Fig. 7, where the tracking error $e_w(t)$ and cost function J_{ESC} are drawn.

The control gains are plotted in Fig. 8. Like Fig. 3, α_I remains close to its initial value, while α_w decreases from 20000 to 8000 before 500s, and decreases further from 8000 to 5000 before 800s.

The motor current I and normalized command U are shown in Fig. 9, with the constraints: $I < I_{max} = 0.85$ and $U < U_{max} = 0.15$ being satisfied.

Finally, to validate the convergence of ESC, we initialize the ULMPC with three different $\alpha_w(0)$ values. Profiles of the control gain α_w are summarized in Fig. 10. Even starting from three different initial conditions, α_w converges to 8000 before 500s, and decreases further from 8000 to 5000 before 800s.

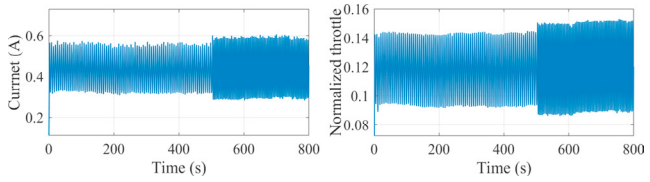

Fig. 9. Motor current and normalized throttle.

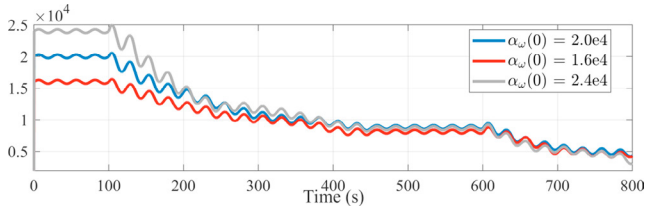

Fig. 10. Convergence of α_w with different initial conditions.

6. CONCLUSIONS

We propose a novel extremum-seeking-based ultra-local model predictive control (ES-ULMPC) by integrating ESC with ULMPC. ESC continuously updates the control gain of the ULMPC online, such that the tracking performance of the ULMPC progressively improves. We implement the ES-ULMPC on a DC motor. Simulation and experimental results demonstrate its enhancement over a ULMPC with constant control gains. ES-ULMPC provides a novel solution for tuning the critical control gain of ULMPC. Future research will focus on comparing the performance of the ES-ULMPC with model-based predictive controllers. More speed profiles from real-world datasets will also be used to further validate the effectiveness of ES-ULMPC.

REFERENCES

Chen, P. and Wang, J. (2015). Nonlinear model predictive control of integrated diesel engine and selective catalytic reduction system for simultaneous fuel economy improvement and emissions reduction. *ASME Transactions Journal of Dynamic Systems, Measurement and Control*, 137(8), 081008–1–13.

Crolla, D.A. and Cao, D. (2012). The impact of hybrid and electric powertrains on vehicle dynamics, control systems and energy regeneration. *Vehicle System Dynamics*, 50(sup1), 95–109.

Doublet, M., Join, C., and Hamelin, F. (2016). Model-free control for unknown delayed systems. In *2016 3rd Conference on Control and Fault-Tolerant Systems (SysTol)*, 630–635. IEEE.

Fliess, M. and Join, C. (2013). Model-free control. *International Journal of Control*, 86(12), 2228–2252.

Fliess, M. and Join, C. (2021). An alternative to proportional-integral and proportional-integral-derivative regulators: Intelligent proportional-derivative regulators. *International Journal of Robust and Nonlinear Control*.

Ghaffari, A., Krstić, M., and Nešić, D. (2012). Multivariable newton-based extremum seeking. *Automatica*, 48(8), 1759–1767.

Hunnekens, B., Di Dino, A., van de Wouw, N., van Dijk, N., and Nijmeijer, H. (2014). Extremum-seeking control for the adaptive design of variable gain controllers. *IEEE Transactions on Control Systems Technology*, 23(3), 1041–1051.

Killingsworth, N.J. and Krstic, M. (2006). Pid tuning using extremum seeking: Online, model-free performance optimization. *IEEE Control Systems Magazine*, 26(1), 70–79.

Krstic, M. and Wang, H.H. (1998). Extremum seeking feedback: Stability proof and application to an aeroengine compressor model. *Automatica*, 36(4), 595–601.

Mboup, M., Join, C., and Fliess, M. (2009). Numerical differentiation with annihilators in noisy environment. *Numerical algorithms*, 50(4), 439–467.

Polack, P., d'Andréa Novel, B., Fliess, M., de La Fortelle, A., and Menhour, L. (2017). Finite-time stabilization of longitudinal control for autonomous vehicles via a model-free approach. *IFAC-PapersOnLine*, 50(1), 12533–12538.

Quirynen, R. and Di Cairano, S. (2020). Presas: Block-structured preconditioning of iterative solvers within a primal active-set method for fast model predictive control. *Optimal Control Applications and Methods*, 41(6), 2282–2307.

Ruoho, S., Kolehmainen, J., Ikaheimo, J., and Arkkio, A. (2009). Interdependence of demagnetization, loading, and temperature rise in a permanent-magnet synchronous motor. *IEEE Transactions on Magnetics*, 46(3), 949–953.

Tran, Q.N., Scholten, J., Ozkan, L., and Backx, A. (2014). A model-free approach for auto-tuning of model predictive control. *IFAC Proceedings Volumes*, 47(3), 2189–2194.

Vafamand, N., Arefi, M.M., Khooban, M.H., Dragičević, T., and Blaabjerg, F. (2018). Nonlinear model predictive speed control of electric vehicles represented by linear parameter varying models with bias terms. *IEEE Journal of Emerging and Selected Topics in Power Electronics*, 7(3), 2081–2089.

Wang, Z., Bai, Y., Wang, J., and Wang, X. (2019). Vehicle path-tracking linear-time-varying model predictive control controller parameter selection considering central process unit computational load. *Journal of Dynamic Systems, Measurement, and Control*, 141(5), 051004.

Wang, Z. and Wang, J. (2020). Ultra-local model predictive control: A model-free approach and its application on automated vehicle trajectory tracking. *Control Engineering Practice*, 101, 104482.

Wang, Z., Zha, J., and Wang, J. (2020). Autonomous vehicle trajectory following: A flatness model predictive control approach with hardware-in-the-loop verification. *IEEE Transactions on Intelligent Transportation Systems*, 22(9), 5613–5623.

Wang, Z., Zhou, X., Shen, H., and Wang, J. (2022a). Algebraic driver steering model parameter identification. *ASME Transactions Journal of Dynamic Systems, Measurement and Control*, 144(5), 051006.

Wang, Z., Zhou, X., and Wang, J. (2022b). Extremum-seeking-based adaptive model-free control and its application to automated vehicle path tracking. *IEEE/ASME Transactions on Mechatronics*, DOI: 10.1109/TMECH.2022.3146727.

Zhao, J. and Wang, J. (2016). Integrated model predictive control of hybrid electric vehicles coupled with aftertreatment systems. *IEEE Transactions on Vehicular Technology*, 65(3), 1199 – 1211.